

Relativistic hyperpolarizabilities of atomic H, Li, and Be^+ systems

Shan-Shan Lu(卢闪闪), Hong-Yuan Zheng(郑弘远), Zong-Chao Yan(严宗朝), James F. Babb, and Li-Yan Tang(唐丽艳)

Citation: Chin. Phys. B, 2025, 34 (**2**): 023202. DOI: 10.1088/1674-1056/ad9911
Journal homepage: http://cpb.iphy.ac.cn; http://iopscience.iop.org/cpb

What follows is a list of articles you may be interested in

Formation of high-density cold molecules via electromagnetic trap

Ya-Bing Ji(纪亚兵), Bin Wei(魏斌), Heng-Jiao Guo(郭恒娇), Qing Liu(刘青), Tao Yang(杨涛), Shun-Yong Hou(侯顺永), and Jian-Ping Yin(印建平)
Chin. Phys. B, 2022, 31 (**10**): 103201. DOI: 10.1088/1674-1056/ac720c

Anisotropic exciton Stark shift in hemispherical quantum dots

Shu-Dong Wu(吴曙东)
Chin. Phys. B, 2021, 30 (**5**): 053201. DOI: 10.1088/1674-1056/abd472

Photoelectron imaging on vibrational excitation and Rydberg intermediate states in multi-photon ionization process of NH_3 molecule

Ya-Nan Sun(孙亚楠), Yan-Hui Wang(王艳辉), Le-Le Song(宋乐乐), Hai-Bin Du(杜海滨), Xiao-Chun Wang(王晓春), Lan-Lai He(赫兰海), Si-Zuo Luo(罗嗣佐), Qin Yang(杨钦), Jing Leng(冷静), Fu-Chun Liu(刘福春)
Chin. Phys. B, 2020, 29 (**9**): 093201. DOI: 10.1088/1674-1056/ab9431

Ellipticity-dependent ionization yield for noble atoms

Hristina Deliba?i?, Violeta Petrovi?
Chin. Phys. B, 2019, 28 (**8**): 083201. DOI: 10.1088/1674-1056/28/8/083201

Quantum photodetachment of hydrogen negative ion in a harmonic potential subjected to static electric field

Azmat Iqbal, Kiran Humayun, Sana Maqsood, Saba Jawaid, Afaq Ahmad, Amin Ur Rahman, Bakht Amin Bacha
Chin. Phys. B, 2019, 28 (**2**): 023201. DOI: 10.1088/1674-1056/28/2/023201

Relativistic hyperpolarizabilities of atomic H, Li, and Be^+ systems

Shan-Shan Lu(卢闪闪)[1,2], Hong-Yuan Zheng(郑弘远)[1,2], Zong-Chao Yan(严宗朝)[3,1], James F. Babb[4], and Li-Yan Tang(唐丽艳)[1,†]

[1] *State Key Laboratory of Magnetic Resonance and Atomic and Molecular Physics, Wuhan Institute of Physics and Mathematics, Innovation Academy for Precision Measurement Science and Technology, Chinese Academy of Sciences, Wuhan* 430071, *China*

[2] *University of Chinese Academy of Sciences, Beijing* 100049, *China*

[3] *Department of Physics, University of New Brunswick, Fredericton, New Brunswick, E3B* 5A3, *Canada*

[4] *ITAMP, Center for Astrophysics | Harvard & Smithsonian,* 60 *Garden St., Cambridge, MA* 02138, *USA*

(Received 6 October 2024; revised manuscript received 13 November 2024; accepted manuscript online 2 December 2024)

For atoms in external electric fields, the hyperpolarizabilities are the coefficients describing the nonlinear interactions contributing to the induced energies at the fourth power of the applied electric fields. Accurate evaluations of these coefficients for various systems are crucial for improving precision in advanced atom-based optical lattice clocks and for estimating field-induced effects in atoms for quantum information applications. However, there is a notable scarcity of research on atomic hyperpolarizabilities, especially in the relativistic realm. Our work addresses this gap by establishing a novel set of alternative formulas for the hyperpolarizability based on the fourth-order perturbation theory. These formulas offer a more reasonable regrouping of scalar and tensor components compared to previous formulas, thereby enhancing their correctness and applicability. To validate our formulas, we perform the calculations for the ground and low-lying excited pure states of few-electron atoms H, Li, and Be^+. The highly accurate results obtained for the H atom could serve as benchmarks for further development of other theoretical methods.

Keywords: hyperpolarizabilities, Stark effect, fourth-order perturbation, few-electron atoms

PACS: 32.60.+i, 32.10.Dk, 31.15.xp, 31.15.ac

DOI: 10.1088/1674-1056/ad9911 **CSTR:** 32038.14.CPB.ad9911

1. Introduction

The response of an atom to an applied electric field is described at leading order by the polarizability (linear response to the field) and at higher order by the hyperpolarizability (nonlinear response to the field). The literature on precision calculations of polarizabilities for atoms[1–5] is extensive compared to that for hyperpolarizabilities, but the methods used to calculate polarizabilities are not necessarily directly applicable to hyperpolarizabilities. Here, our intent is to present a theoretical formalism and some highly-accurate benchmark values for hyperpolarizabilities of few-electron atoms.

Hyperpolarizabilities[6–8] are the coefficients describing the response induced in atoms at the order of the fourth power of applied electric fields (and describe induced dipole moments at the third power of applied electric fields). As perturbative corrections to the energies of atoms in electric fields, the relative values of the hyperpolarizabilities compared to the values of the polarizabilities (which appear at the second power of applied electric fields) are fundamental to estimating the impact of field intensities on nonlinear phenomena.[9,10] Knowledge of the values of hyperpolarizabilities plays a crucial role in arrangements to suppress nonlinear effects for precision laser spectroscopy measurements,[11–14] especially in the pursuit and development of ever higher-precision optical clocks.[15–18] Moreover, applications of highly excited Rydberg states in neutral atom quantum computing are rapidly developing and it is reasonable to expect that improvements in quantification of hyperpolarizabilities will be needed as control of these atoms in electric fields is sought [see, for example, Eq. (11) of Ref. [19]].

In this study, we present a set of general formulas for the atomic hyperpolarizabilities, which improves our previously published theory[20] by offering a more reasonable regrouping of the scalar and tensor components, thus preserving the common understanding of the relativistic correction being small. The utility of the new formulas is demonstrated by conducting high-accuracy calculations on H, Li, and Be^+ using both nonrelativistic and relativistic approaches. For the H atom in an excited state, we exclude all degenerate states when calculating the hyperpolarizabilities.[21] These so-called pure state hyperpolarizabilities can serve as benchmarks for testing computational methods. For the Li and Be^+ systems, we leverage the nonrelativistic numerical values obtained using our previous theory,[20,22] demonstrating the correctness and applicability of the present formulas.

Atomic units (a.u.), where $e = 1$, $a_0 = 1$, and $\hbar = 1$, are used throughout; the a.u. of the (second) hyperpolarizability is $e^4 a_0^4 / E_\mathrm{h}^3$ ($\sim 6.235\,379\,9905(38) \times 10^{-65}$ $\mathrm{C}^4 \cdot \mathrm{m}^4 \cdot \mathrm{J}^{-3}$), where e is the electron charge, a_0 is the Bohr radius, and $E_\mathrm{h} = e^2/a_0$ is the Hartree.

†Corresponding author. E-mail: lytang@apm.ac.cn

© 2025 Chinese Physical Society and IOP Publishing Ltd. All rights, including for text and data mining, AI training, and similar technologies, are reserved.

2. An alternative formula

When an atom is placed in a uniform external electric field, its energy levels change due to the influence of the field. Specifically, the energy at second order in the electric field depends on the atomic dipole polarizability. The fourth-order shift depends on the atomic hyperpolarizability γ and can be expressed in the form

$$\Delta E_4 = -\frac{\varepsilon^4}{24}\gamma = -\frac{\varepsilon^4}{24}\left\{\gamma_0 + g_2(J,M_J)\gamma_2 + \left[g_4(J,M_J)\gamma_4^{(1)} + g_2^2(J,M_J)\gamma_4^{(2)}\right]\right\}, \tag{1}$$

where ε is the electric field strength, the coefficients $g_2(J,M_J)$ and $g_4(J,M_J)$ depend on the magnetic quantum number M_J,

$$g_2(J,M_J) = \begin{cases} 0, & J \le \dfrac{1}{2}, \\ \dfrac{3M_J^2 - J(J+1)}{J(2J-1)}, & \text{otherwise}, \end{cases} \tag{2}$$

$$g_4(J,M_J) = \begin{cases} 0, & J \le \dfrac{3}{2}, \\ \dfrac{3(5M_J^2 - J^2 - 2J)(5M_J^2 + 1 - J^2) - 10M_J^2(4M_J^2 - 1)}{J(2J-1)(2J-2)(2J-3)}, & \text{otherwise}. \end{cases} \tag{3}$$

Also in Eq. (1), γ_0 corresponds to the scalar component of the hyperpolarizability, whereas γ_2, $\gamma_4^{(1)}$, and $\gamma_4^{(2)}$ correspond to the tensor components, which have the following forms:

$$\begin{aligned}\gamma_0 &= (-1)^{2J}\frac{24}{\sqrt{2J+1}}\sum_{J_aJ_bJ_c}\mathcal{G}_0^{(1)}(J,J_a,J_b,J_c)\mathcal{T}_1(J_a,J_b,J_c) \\ &\quad - \frac{24}{2J+1}\sum_{J_aJ_c}\mathcal{G}_{00}^{(2)}(J,J_a,J_c)\mathcal{T}_2(J_a,J_c),\end{aligned} \tag{4}$$

$$\begin{aligned}\gamma_2 &= (-1)^{2J}24\sqrt{\frac{J(2J-1)}{(2J+3)(J+1)(2J+1)}} \\ &\quad \times \sum_{J_aJ_bJ_c}\mathcal{G}_2^{(1)}(J,J_a,J_b,J_c)\mathcal{T}_1(J_a,J_b,J_c) \\ &\quad - \frac{24}{2J+1}\sqrt{\frac{J(2J-1)}{(2J+3)(J+1)}} \\ &\quad \times \sum_{J_aJ_c}[\mathcal{G}_{02}^{(2)}(J,J_a,J_c) + \mathcal{G}_{20}^{(2)}(J,J_a,J_c)]\mathcal{T}_2(J_a,J_c),\end{aligned} \tag{5}$$

$$\begin{aligned}\gamma_4^{(1)} &= (-1)^{2J}24\sqrt{\frac{J(2J-1)(J-1)(2J-3)}{(2J+5)(J+2)(2J+3)(J+1)(2J+1)}} \\ &\quad \times \sum_{J_aJ_bJ_c}\mathcal{G}_4^{(1)}(J,J_a,J_b,J_c)\mathcal{T}_1(J_a,J_b,J_c),\end{aligned} \tag{6}$$

$$\begin{aligned}\gamma_4^{(2)} &= -\frac{24J(2J-1)}{(2J+3)(2J+1)(J+1)} \\ &\quad \times \sum_{J_aJ_c}\mathcal{G}_{22}^{(2)}(J,J_a,J_c)\mathcal{T}_2(J_a,J_c),\end{aligned} \tag{7}$$

where $\mathcal{T}_1(J_a,J_b,J_c)$ and $\mathcal{T}_2(J_a,J_c)$ are defined in Appendix A by Eqs. (A9) and (A10), $\mathcal{G}_\lambda^{(1)}(J,J_a,J_b,J_c)$ with $\lambda = 0,2,4$ and $\mathcal{G}_{k_1k_2}^{(2)}(J,J_a,J_c)$ are defined in Appendix A by Eqs. (A18) and (A19). The detailed derivation of Eq. (1) is provided in Appendix A. This formula (1) features a distinct partitioning, in terms of both scalar and tensor components, compared to the commonly used one in Refs. [10,20], while still yielding the same total hyperpolarizability γ.

3. Computational methods

3.1. Single-electron Schrödinger and Dirac equations

When solving the hydrogen, the nuclear mass is set to be infinite, and the point nucleus model is adopted. For the nonrelativistic case, the Schrödinger equation for hydrogen is given by

$$\left[-\frac{1}{2}\nabla^2 + V(r)\right]\psi_{\rm S}(\boldsymbol{r}) = E_{\rm S}\psi_{\rm S}(\boldsymbol{r}), \tag{8}$$

where $V(r) = -Z/r$ and Z is the nuclear charge. Due to its rotational symmetry, there exist solutions to Eq. (8) of the separable form

$$\psi_{\rm S}(\boldsymbol{r}) = U_{nl}(r)Y_{lm}(\theta,\phi), \tag{9}$$

where $Y_{lm}(\theta,\phi)$ is a spherical harmonic function and the radial function $U_{nl}(r)$ satisfies the differential equation

$$\left[-\frac{1}{2}\frac{{\rm d}^2}{{\rm d}r^2} - \frac{1}{r}\frac{\rm d}{{\rm d}r} + \frac{l(l+1)}{2r^2} + V(r)\right]U_{nl}(r) = E_{\rm S}U_{nl}(r). \tag{10}$$

For the relativistic case, the Dirac equation for hydrogen is given by

$$\left[c\boldsymbol{\alpha}\cdot\boldsymbol{p} + \beta c^2 + V(r)\right]\psi_{\rm D}(\boldsymbol{r}) = E_{\rm D}\psi_{\rm D}(\boldsymbol{r}), \tag{11}$$

where $c = 137.035999084$ is the speed of light,[23] $\boldsymbol{p}$ is the momentum operator, and $\boldsymbol{\alpha}$ and β are the usual 4×4 Dirac matrices.[24] The solutions to Eq. (11) can be expressed in the following separable form:

$$\psi_{\rm D}(\boldsymbol{r}) = \frac{1}{r}\begin{pmatrix} {\rm i}P_{n\kappa}(r)\Omega_{\kappa m}(\hat{\boldsymbol{r}}) \\ Q_{nk}(r)\Omega_{-\kappa m}(\hat{\boldsymbol{r}}) \end{pmatrix}, \tag{12}$$

where $P_{n\kappa}(r)$ and $Q_{n\kappa}(r)$ are the large and small components of the radial function, and $\Omega_{\kappa m}(\hat{\boldsymbol{r}})$ and $\Omega_{-\kappa m}(\hat{\boldsymbol{r}})$ are the angular components. By substituting Eq. (12) into Eq. (11), we

obtain the following coupled first-order differential equations that describe the behavior of $P_{n\kappa}(r)$ and $Q_{n\kappa}(r)$:

$$\begin{pmatrix} V(r) & c\left(\frac{\mathrm{d}}{\mathrm{d}r}-\frac{\kappa}{r}\right) \\ -c\left(\frac{\mathrm{d}}{\mathrm{d}r}+\frac{\kappa}{r}\right) & -2c^2+V(r) \end{pmatrix} \begin{pmatrix} P_{n\kappa}(r) \\ Q_{n\kappa}(r) \end{pmatrix} = E \begin{pmatrix} P_{n\kappa}(r) \\ Q_{n\kappa}(r) \end{pmatrix}, \quad (13)$$

where $E = E_{\mathrm{D}} - c^2$.

While it is possible to solve the Schrödinger equation (10) and the Dirac equation (13) analytically, in this study, we choose to solve them numerically using B-spline functions within a specific cavity.[2,25–27] This approach enables us to validate our numerical method, which will be subsequently used to diagonalize the Hamiltonian. For example, by using the complete B-spline basis, we can express $U_{nl}(r)$ as a discrete sum of N-dimensional, k-order B-spline basis functions

$$U_{nl}(r) = \sum_{i=1}^{N} c_i B_i^k(r). \quad (14)$$

The function $B_i^k(r)$ is non-zero only within the knot intervals $t_i \le r \le t_{i+k}$, where t_i represents the knot sequence. In the nonrelativistic case, the radial wave functions must satisfy the boundary conditions $U_{nl}(0) = U_{nl}(R) = 0$, where R is the radius of the cavity. In the relativistic case, the Notre Dame (ND) boundary conditions[25,28] of $P_{n\kappa}(0) = 0$ and $P_{n\kappa}(R) = Q_{n\kappa}(R)$ are imposed to address the issues related to the "Klein Paradox". In order to obtain accurate bound-state wave functions, it is more appropriate to use an exponential knot distribution for $B_i^k(r)$ given by

$$t_{i+k-1} = R \times \frac{\exp\left[\eta\left(\frac{i-1}{n-1}\right)\right]-1}{\exp(\eta)-1}, \quad i = 1,2,\ldots,N-k+2. \quad (15)$$

Here, $\eta = a \times R$ is an adjustable exponential knot parameter. In the present work, the radii of the confining cavity are fixed at $R = 400$ a.u. and $R = 600$ a.u. for nonrelativistic and relativistic calculations, respectively. The value of a is optimized by reproducing the exact energies[29] of low-lying states up to 20 significant digits.

3.2. DFCP method

Since the Li atom and Be^+ ion can be regarded as a frozen core combined with one valence electron, these systems can be solved using the Dirac–Fock plus core polarization (DFCP) method.[25,27] As described in previous studies,[30–32] the initial step in the DFCP method is to perform a Dirac–Fock calculation of the frozen core. For monovalent electron systems, the effective Hamiltonian can be written as

$$h_{\mathrm{DFCP}}(\boldsymbol{r}) = c\boldsymbol{\alpha}\cdot\boldsymbol{p} + (\beta-1)c^2 + V(r) + V_{\mathrm{dir}}(r) + V_{\mathrm{exc}}(r) + V_1(r). \quad (16)$$

Here, $V_{\mathrm{dir}}(r)$ and $V_{\mathrm{exc}}(r)$ are the direct and exchange potentials between the core electrons and the valence electron, respectively, and $V_1(r)$ is the semiempirical polarization potential,

$$V_1(r) = -\frac{\alpha_{\mathrm{core}}}{2r^4}\left[1-\exp\left(-\frac{r^6}{\rho_\kappa^6}\right)\right], \quad (17)$$

where α_{core} is the core dipole polarizability, ρ_κ is the cutoff parameter, and κ is the angular quantum number. In the present work, we use $\alpha_{\mathrm{core}} = 0.1894$ a.u. for Li^+ and $\alpha_{\mathrm{core}} = 0.05182$ a.u. for Be^{2+}.[33] The cutoff parameter ρ_κ is fine-tuned to accurately replicate the experimental energy of the lowest state associated with each value of κ.

4. Results and discussion

4.1. Hydrogen

Table 1 presents a convergence analysis of the nonrelativistic and relativistic hyperpolarizabilities, γ_0, for the ground state of the hydrogen atom. As the number of B-spline basis functions N varies from 100 to 400, the nonrelativistic value gradually approaches the exact value of $10665/8 = 1333.125$ a.u.[34] Additionally, the relativistic result has been accurately determined to 21 significant figures. The extrapolated value can be obtained by assuming that the ratio of two successive hyperpolarizability differences remains constant as N tends to infinity. Comparing the nonrelativistic and relativistic values, we find that the relativistic correction to the ground-state hyperpolarizability is $-0.135\,342\,240\,716\,897\,63$ a.u.

The convergence of calculations for the nonrelativistic 2p and 3d states, as the size of the B-spline basis set N increases, is presented in Tables B1 and B2 of Appendix B. It can be observed that the scalar and tensor components have converged to at least 21 significant digits. Specifically, for the 2p ($|M_L| = 1$) state, the total hyperpolarizability γ is determined as 5 326 848 a.u. by utilizing Eqs. (1)–(3), which aligns perfectly with the result reported in Ref. [35]. It is worth reiterating that in our calculations, we have excluded all degenerate states by considering only the pure state hyperpolarizabilities,[21] as shown in Eqs. (A9) and (A10) of Appendix A.

In the relativistic case, the hyperpolarizabilities of $2p_{1/2}$ and $2p_{3/2}$ states have been calculated up to 21 significant digits, as shown in Table B3 of Appendix B. These values, when compared to the nonrelativistic results, have decreased due to the relativistic corrections. Specifically, the relativistic correction for the scalar component γ_0 of the $2p_{1/2}$ state is $-1079.819\,152\,781\,342\,11$ a.u., while for the $2p_{3/2}$ state it is $-58.946\,729\,464\,319\,25$ a.u. Additionally, for the tensor components γ_2 and $\gamma_4^{(2)}$ of the $2p_{3/2}$ state, these corrections are $-93.818\,725\,858\,667\,39$ a.u. and $-1.166\,186\,367\,213\,346\,6$ a.u., respectively. For the $3d_{3/2}$ and $3d_{5/2}$ states, as presented in Tables B4 and B5 of Appendix B, the hyperpolarizabilities have been determined with an accuracy of more than 19 significant digits. The differences relative to the nonrelativistic γ_0 are $-42\,365.011\,332\,071\,4$ a.u. for the $3d_{3/2}$ state and $-10\,610.289\,079\,484\,2$ a.u. for the $3d_{5/2}$ state. Notably, the tensor components γ_2, $\gamma_4^{(1)}$, and $\gamma_4^{(2)}$ of the $3d_{5/2}$ state closely approximate the nonrelativistic results. All the final values of γ_0, γ_2, $\gamma_4^{(1)}$, and $\gamma_4^{(2)}$ are summarized in Table 2.

Table 1. Convergence of the nonrelativistic and relativistic hyperpolarizability γ_0 for the ground state of the H atom, as the size of basis set N increases progressively, in atomic units. It should be noted that N represents the number of intermediate states with different quantum numbers, and since these numbers are all the same, we use only N to uniformly identify them.

Nonrelativistic		Relativistic	
N	γ_0	N	γ_0
100	1 333.125 000 000 004	100	1 332.989 657 756
150	1 333.125 000 000 000 023	200	1 332.989 657 759 283 081
200	1 333.125 000 000 000 000 65	300	1 332.989 657 759 283 102 377
250	1 333.125 000 000 000 000 041	400	1 332.989 657 759 283 102 385
300	1 333.125 000 000 000 000 004 4	500	1 332.989 657 759 283 102 376
350	1 333.125 000 000 000 000 000 67	600	1 332.989 657 759 283 102 372
400	1 333.125 000 000 000 000 000 13	Extrap.	1 332.989 657 759 283 102 370
Extrap.	1 333.125 000 000 000 000 000 05		
Ref. [34]	1 333.125		

Table 2. Summary of nonrelativistic and relativistic pure state hyperpolarizabilities for the low-lying states of the H atom, in atomic units. All the tabulated digits are insensitive to further enlargement of the B-spline basis functions. The numbers in the square brackets denote powers of 10.

State	γ_0	γ_2	$\gamma_4^{(2)}$	$\gamma_4^{(1)}$
		Nonrelativistic		
1s	1333.125			
2p	8.130 560[6]	−2.769 472[6]	−3.424[4]	
3d	1.913 524 179 3[9]	−1.027 110 959 357 142 857 142[9]	−6.944 162 4[7]	2.939 248 330 714 285 714 28[7]
		Relativistic		
$1s_{1/2}$	1 332.989 657 759 283 102 37			
$2p_{1/2}$	8.129 480 180 847 218 657 89[6]			
$2p_{3/2}$	8.130 501 053 270 535 680 75[6]	−2.769 565 818 725 858 667 39[6]	−3.424 116 618 636 721 334 66[4]	
$3d_{3/2}$	1.913 481 814 288 667 928 6[9]	−7.189 813 879 847 891 582 0[8]	−3.402 556 953 695 351 845 4[7]	
$3d_{5/2}$	1.913 513 569 010 920 515 8[9]	−1.027 113 325 161 421 946 0[9]	−6.944 098 825 526 114 424 3[7]	2.939 326 812 562 169 711 9[7]

4.2. Li atom and Be^+ ion

We have recalculated the nonrelativistic hyperpolarizabilities of the Li atom and Be^+ ion in their low-lying states, in the framework of the Hylleraas variational method using the formulas presented in Section 2. More information on the computational methodology and convergence studies can be found in our previous publications.[5,20,22] For the relativistic hyperpolarizabilities, we employed the DFCP method. Specifically, we performed single-electron calculations for the relativistic hyperpolarizabilities of Li and Be^+ using a frozen-core Hamiltonian and a semiempirical polarization potential as detailed in Subsection 3.2. To ensure accuracy, we substituted our energies with the corresponding NIST data,[36] resulting in errors primarily originating from the theoretical reduced matrix elements. By comparing these matrix elements with the values in Ref. [37], we observed relative differences within 0.3% and 0.2% for Li and Be^+, respectively. To conservatively estimate the uncertainties in the relativistic hyperpolarizabilities, we introduced fluctuations of 0.3% and 0.2%, respectively, into all the reduced matrix elements. The present nonrelativistic (Hylleraas) and relativistic (DFCP) results are listed in Tables 3 and 4.

From the comparison of Hylleraas and DFCP results presented in Tables 3 and 4, it is clear that they generally agree with each other except for the ground state of Li atom. There exists a significant discrepancy between the DFCP result of 5750 a.u. and the Hylleraas result of 3060(40) a.u., which can be attributed to a numerical cancellation of DFCP result. In the case of the hyperpolarizability of the $2s_{1/2}$ state, it is determined as the sum of nine distinct types of intermediate states. These intermediate states can be further categorized based on their orbital angular quantum numbers, denoted as $(m,n,k) = (mp_j, ns_{1/2}, kp_j)$ and $(mp_j, nd_{j'}, kp_j)$, where $j = 1/2, 3/2$, $j' = 3/2, 5/2$, and $|j - j'| \leq 1$. The contributions from $(mp_j, ns_{1/2}, kp_j)$ and $(mp_j, nd_{j'}, kp_j)$ are $-1\,469\,773$ a.u. and $1\,475\,523$ a.u., respectively. As a result of this cancellation, there is a loss of three significant figures when combining the two contributions to obtain the total γ_0. Consequently, we can only provide the central value of 5750 a.u., which has the same order of magnitude as the nonrelativistic result. However, this situation does not arise for the ground state of Be^+. The contributions from $(mp_j, ns_{1/2}, kp_j)$ and $(mp_j, nd_{j'}, kp_j)$ amount to -20263 a.u. and 8755 a.u., respectively, and their sum equals $-11508(92)$ a.u., which is in good agreement with the all-order result of $-11496(6)$ a.u. as reported in Ref. [38].

Table 3. Nonrelativistic and relativistic hyperpolarizabilities of the low-lying states of the Li atom, in atomic units. The numbers in parentheses denote computational uncertainty, while the numbers in square brackets represent the power of 10.

State	γ_0	γ_2	$\gamma_4^{(2)}$	$\gamma_4^{(1)}$
		Nonrelativistic (Hylleraas)		
2s	3060(40)			
2p	9.9854(4)[6]	−6.2074(4)[6]	1.5539(2)[4]	
3d	9.38618(1)[11]	−1.93402(1)[12]	1.01218(1)[12]	−1.5938(6)[10]
		Relativistic (DFCP)		
$2s_{1/2}$	5750			
$2p_{1/2}$	9.82(12)[6]			
$2p_{3/2}$	9.82(12)[6]	−6.126(74)[6]	1.439(17)[4]	
$3d_{3/2}$	9.37(12)[11]	−1.351(17)[12]	4.948(60)[11]	
$3d_{5/2}$	9.37(12)[11]	−1.930(23)[12]	1.009(13)[12]	−1.582(19)[10]

Table 4. Nonrelativistic and relativistic hyperpolarizabilities of the low-lying states of the Be^+ ion, in atomic units. The numbers in parentheses denote computational uncertainty, while the numbers in square brackets represent the power of 10.

State	γ_0	γ_2	$\gamma_4^{(2)}$	$\gamma_4^{(1)}$
		Nonrelativistic (Hylleraas)		
2s	−11521.30(3)			
2p	6.64785(2)[3]	−5.24075(4)[3]	2.13286(2)[3]	
3d	5.9851(2)[8]	−1.3038(4)[9]	7.6397(2)[8]	−5.7795(4)[7]
		Relativistic (DFCP)		
$2s_{1/2}$	−11508(92)			
Ref. [38]	−11496(6)			
$2p_{1/2}$	6.647(54)[3]			
$2p_{3/2}$	6.650(53)[3]	−5.237(42)[3]	2.134(17)[3]	
$3d_{3/2}$	5.952(48)[8]	−9.081(73)[8]	3.730(30)[8]	
$3d_{5/2}$	5.966(48)[8]	−1.301(11)[9]	7.638(61)[8]	−5.835(47)[7]

4.3. Comparison of two sets of formulas

The nonrelativistic and relativistic scalar and tensor components of hyperpolarizability, as presented in Tables 2–4, exhibit minimal differences when calculated using the current formula in Eq. (1), as generally accepted that the relativistic effects are small. In contrast, for the previous formula described in Refs. [10,20], this does not hold true, as demonstrated in Fig. 1 for the 2p state of Li and Be^+, although the total hyperpolarizability γ remains the same.

The numerical exemplification pertinent to the aforementioned point can be referenced by examining the values of Be^+ in the 2p state, as presented in Table 5. According to the previous formula,[10,20] the nonrelativistic value of γ_0 is 10913.57(1) a.u., and the corresponding relativistic corrections are −2130(70) a.u. (20%), resulting in $\gamma_0(2p_{3/2}) = 8784(70)$ a.u., and −4267(54) a.u. (39%), resulting in $\gamma_0(2p_{1/2}) = 6647(54)$ a.u. On the other hand, using the present formula, the relativistic corrections on γ_0 are within the error bars and can be estimated as approximately 0.01%. Similarly, the relativistic correction on γ_2 using the previous formula is 2137(42) a.u. (29%), which is significantly larger than the estimated 0.08% correction obtained from the present formula. Nevertheless, regardless of the magnetic sublevel considered, the overall hyperpolarizability γ obtained from both formulas remains consistent. These comparisons indicate that the present formula is more preferable in defining the scalar and tensor components of the hyperpolarizability compared to the previous formula,[10,20] especially considering that relativistic effects on physical properties are typically small.

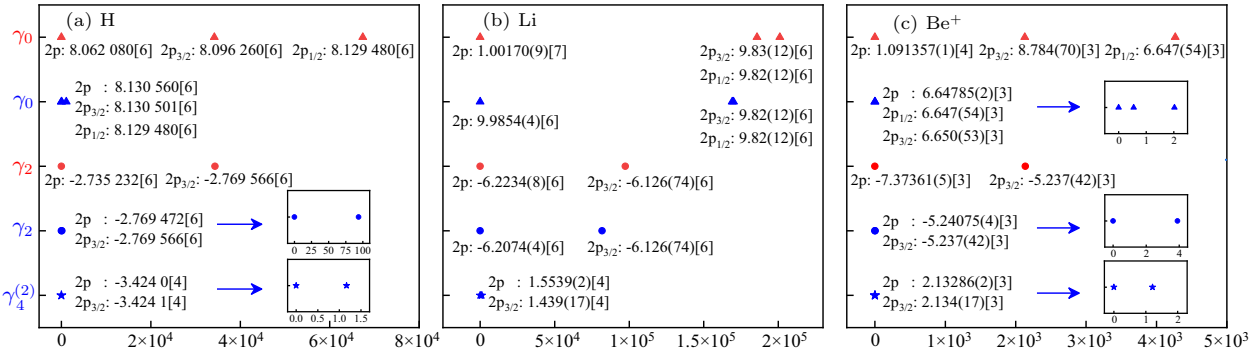


Fig. 1. Comparison of the present and previous[20] relativistic corrections on the scalar and tensor hyperpolarizabilities for the 2p state of H, Li and Be^+, where the values calculated using the previous formula from Ref. [20] are shown in red, while the values calculated using the present formula Eq. (1) are shown in blue. Also γ_0, γ_2, and $\gamma_4^{(2)}$ are denoted by filled triangles, circles, and stars, respectively. All the data are referenced to the nonrelativistic results on the far left, and the horizontal axis represents the absolute value of relativistic corrections. The inserts provide a zoomed-in view of the overlapping points within the main image.

Table 5. Comparison of hyperpolarizabilities for the nonrelativistic 2p and relativistic $2p_{3/2}$ states of the Be^+ ion, performed using the present formula (1) and the previous formula (27) of Ref. [20]. The numbers in parentheses indicate the computational uncertainty. In atomic units.

State		γ_0	γ_2	$\gamma_4^{(2)}$	g_2		g_2^2		$\gamma(M_L=0)$	$\gamma(\lvert M_L\rvert=1)$
					$M_L=0$	$\lvert M_L\rvert=1$	$M_L=0$	$\lvert M_L\rvert=1$		
2p	Present	6647.85(2)	−5240.75(4)	2132.86(2)	−2	1	4	1	25660.79(5)	3539.96(5)
	Previous[20]	10913.57(1)	−7373.61(5)		−2	1			25660.79(5)	3539.96(5)
					$\lvert M_J\rvert=1/2$	$\lvert M_J\rvert=3/2$	$\lvert M_J\rvert=1/2$	$\lvert M_J\rvert=3/2$	$\gamma(\lvert M_J\rvert=1/2)$	$\gamma(\lvert M_J\rvert=3/2)$
$2p_{3/2}$	Present	6650(53)	−5237(42)	2134(17)	−1	1	1	1	14021(70)	3547(70)
	Previous[20]	8784(70)	−5237(42)		−1	1			14021(82)	3547(82)

5. Conclusion

In conclusion, we have developed a new formula to calculate the atomic hyperpolarizability, which provides a better separation of scalar and tensor components. This alternative formula has been applied to compute the hyperpolarizabilities for low-lying states of the H, Li, and Be^+ systems, both in nonrelativistic and relativistic regimes. Our numerical analysis demonstrates that the relativistic corrections to the scalar and tensor components are not significantly different from their nonrelativistic counterparts, unlike what the previous formula[10,20] suggests.

Appendix A: Derivation of the hyperpolarizability

In our previous work, which is referenced as Ref. [20], we derived the hyperpolarizability. However, we unintentionally overlooked a crucial constraint involving the Kronecker $\delta(n,0)$. This constraint is necessary when dealing with the second intermediate states $|n\rangle$ with the initial state $|0\rangle$ in the second term of the fourth-order energy correction ΔE_4, as shown in Eqs. (A34) and (A35) of Ref. [20]. In this appendix, we will revisit the derivation process from the beginning, taking into account the presence of the $\delta(n,0)$ constraint. Remarkably, we have discovered that the new formula we derived is in complete agreement with the previous one, despite having different partitioning in terms of "γ" components.

The Hamiltonian of an atom under the influence of a weak external electric field is given by

$$H = H_0 + H' = H_0 - \boldsymbol{\varepsilon}\cdot\boldsymbol{d}. \tag{A1}$$

Here, H_0 is the atom's unperturbed Hamiltonian, $\boldsymbol{\varepsilon}$ is the electric field strength, and $\boldsymbol{d}$ is the atom's electric dipole moment, given by $\boldsymbol{d} = -e\boldsymbol{r}$, where $\boldsymbol{r}$ is the electron's position vector relative to a laboratory frame. The perturbation, H', can be expressed as $\boldsymbol{r}\cdot\boldsymbol{\varepsilon}$ in atomic units. It is noted that the electric quadrupole and magnetic dipole interactions have been omitted from Eq. (A1), and the treatment of these higher-order terms can be found in Refs. [39,40].

According to perturbation theory, the fourth-order energy shift[10] contains two terms $\Delta E_4^{(1)}$ and $\Delta E_4^{(2)}$,

$$\begin{aligned}\Delta E_4 &= \Delta E_4^{(1)} + \Delta E_4^{(2)} \\ &= \sum_{mnk} \frac{\langle 0|H'|m\rangle\langle m|H'|n\rangle\langle n|H'|k\rangle\langle k|H'|0\rangle}{(E_0-E_m)(E_0-E_n)(E_0-E_k)} \\ &\quad - \sum_{mk} \frac{\langle 0|H'|m\rangle\langle m|H'|0\rangle\langle 0|H'|k\rangle\langle k|H'|0\rangle}{(E_0-E_m)(E_0-E_k)^2}.\end{aligned} \tag{A2}$$

Using the spherical tensor operator technique, we can expand $H'|n\rangle\langle n|H'$ of Eq. (A2) as

$$H'|n\rangle\langle n|H' = \sum_{Kq}(-1)^{K+q}[r^{(1)}\otimes\lambda_n r^{(1)}]_q^K[\boldsymbol{\varepsilon}^{(1)}\otimes\boldsymbol{\varepsilon}^{(1)}]_{-q}^K, \tag{A3}$$

where $r_\mu^{(1)} = \sqrt{\frac{4\pi}{3}}rY_{1\mu}$ and $\lambda_n = |n\rangle\langle n|$. Assuming that the external electric field $\boldsymbol{\varepsilon}$ is linearly polarized parallel to the z axis, only the $q=0$ component exists in Eq. (A3). Thus we have

$$\begin{aligned}H'|n\rangle\langle n|H' &= \sum_K (-1)^K\sqrt{2K+1} \\ &\quad\times\sum_{q_1q_2}\begin{pmatrix}1 & 1 & K\\ q_1 & q_2 & 0\end{pmatrix} r_{q_1}^{(1)}\lambda_n r_{q_2}^{(1)}[\boldsymbol{\varepsilon}^{(1)}\otimes\boldsymbol{\varepsilon}^{(1)}]_0^K.\end{aligned} \tag{A4}$$

Substituting Eq. (A4) into Eq. (A2), $\Delta E_4^{(1)}$ and $\Delta E_4^{(2)}$ can be written as

$$\begin{aligned}\Delta E_4^{(1)} &= \sum_{mnk}\sum_{k_1k_2}\sum_{q_1q_2q_3q_4}(-1)^{k_1+k_2}\sqrt{(2k_1+1)(2k_2+1)} \\ &\quad\times\begin{pmatrix}1 & 1 & k_1\\ q_1 & q_2 & 0\end{pmatrix}\begin{pmatrix}1 & 1 & k_2\\ q_3 & q_4 & 0\end{pmatrix} \\ &\quad\times[\boldsymbol{\varepsilon}^{(1)}\otimes\boldsymbol{\varepsilon}^{(1)}]_0^{k_1}[\boldsymbol{\varepsilon}^{(1)}\otimes\boldsymbol{\varepsilon}^{(1)}]_0^{k_2} \\ &\quad\times\frac{\langle 0|r_{q_1}^{(1)}|m\rangle\langle m|r_{q_2}^{(1)}|n\rangle\langle n|r_{q_3}^{(1)}|k\rangle\langle k|r_{q_4}^{(1)}|0\rangle}{(E_0-E_m)(E_0-E_n)(E_0-E_k)},\end{aligned} \tag{A5}$$

$$\begin{aligned}\Delta E_4^{(2)} &= -\sum_m\sum_{k_1}\sum_{q_1q_2}(-1)^{k_1}\sqrt{2k_1+1}\begin{pmatrix}1 & 1 & k_1\\ q_1 & q_2 & 0\end{pmatrix} \\ &\quad\times\frac{\langle 0|r_{q_1}^{(1)}|m\rangle\langle m|r_{q_2}^{(1)}|0\rangle}{(E_0-E_m)}[\boldsymbol{\varepsilon}^{(1)}\otimes\boldsymbol{\varepsilon}^{(1)}]_0^{k_1} \\ &\quad\times\sum_k\sum_{k_2}\sum_{q_3q_4}(-1)^{k_2}\sqrt{2k_2+1}\begin{pmatrix}1 & 1 & k_2\\ q_3 & q_4 & 0\end{pmatrix} \\ &\quad\times\frac{\langle 0|r_{q_3}^{(1)}|k\rangle\langle k|r_{q_4}^{(1)}|0\rangle}{(E_0-E_k)^2}[\boldsymbol{\varepsilon}^{(1)}\otimes\boldsymbol{\varepsilon}^{(1)}]_0^{k_2},\end{aligned} \tag{A6}$$

where all the initial and intermediate states are simply denoted as $|0\rangle = |n_0JM_J\rangle$, $|m\rangle = |mJ_aM_a\rangle$, $|n\rangle = |nJ_bM_b\rangle$, $|k\rangle = |kJ_cM_c\rangle$, with n_0, m, n, and k being the corresponding principal quantum numbers of states. The summation in Eqs. (A5) and (A6) over m, n, and k actually represents the summation over all three sets of quantum numbers $\{m,J_a,M_a\}$, $\{n,J_b,M_b\}$, and $\{k,J_c,M_c\}$.

By utilizing the Wigner–Eckart theorem to simplify Eqs. (A5) and (A6), we can arrive at the following expressions:

$$\begin{aligned}\Delta E_4^{(1)} &= -\sum_{J_aJ_bJ_c}\sum_{k_1k_2}(-1)^{k_1+k_2}\sqrt{(2k_1+1)(2k_2+1)} \\ &\quad\times[\boldsymbol{\varepsilon}^{(1)}\otimes\boldsymbol{\varepsilon}^{(1)}]_0^{k_1}[\boldsymbol{\varepsilon}^{(1)}\otimes\boldsymbol{\varepsilon}^{(1)}]_0^{k_2}\mathcal{C}_1\mathcal{T}_1(J_a,J_b,J_c),\end{aligned} \tag{A7}$$

$$\begin{aligned}\Delta E_4^{(2)} &= \sum_{J_aJ_c}\sum_{k_1k_2}(-1)^{k_1+k_2}\sqrt{(2k_1+1)(2k_2+1)} \\ &\quad\times[\boldsymbol{\varepsilon}^{(1)}\otimes\boldsymbol{\varepsilon}^{(1)}]_0^{k_1}[\boldsymbol{\varepsilon}^{(1)}\otimes\boldsymbol{\varepsilon}^{(1)}]_0^{k_2}\mathcal{C}_2\mathcal{T}_2(J_a,J_c),\end{aligned} \tag{A8}$$

where $\mathcal{T}_1(J_a,J_b,J_c)$ and $\mathcal{T}_2(J_a,J_c)$ are radial-dependent terms, $\mathcal{C}_1$ and $\mathcal{C}_2$ are the angular coefficients. The explicit expressions are as follows:

$$\mathcal{T}_1(J_a,J_b,J_c) = \sum_{mnk}{}' \frac{\langle n_0J\|r^{(1)}\|mJ_a\rangle\langle mJ_a\|r^{(1)}\|nJ_b\rangle\langle nJ_b\|r^{(1)}\|kJ_c\rangle\langle kJ_c\|r^{(1)}\|n_0J\rangle}{\left[E_k(J_c)-E_{n_0}(J)\right]\left[E_m(J_a)-E_{n_0}(J)\right]\left[E_n(J_b)-E_{n_0}(J)\right]}, \tag{A9}$$

$$\mathcal{T}_2(J_a,J_c) = \sum_m{}' \frac{\langle n_0J\|r^{(1)}\|mJ_a\rangle\langle mJ_a\|r^{(1)}\|n_0J\rangle}{\left[E_m(J_a)-E_{n_0}(J)\right]}\sum_k{}' \frac{\langle n_0J\|r^{(1)}\|kJ_c\rangle\langle kJ_c\|r^{(1)}\|n_0J\rangle}{\left[E_k(J_c)-E_{n_0}(J)\right]^2}, \tag{A10}$$

$$\mathcal{C}_1 = \sum_{M_a M_b M_c} \sum_{q_1 q_2 q_3 q_4} (-1)^{J-M_J+J_a-M_a+J_b-M_b+J_c-M_c} \begin{pmatrix} 1 & 1 & k_1 \\ q_1 & q_2 & 0 \end{pmatrix} \begin{pmatrix} 1 & 1 & k_2 \\ q_3 & q_4 & 0 \end{pmatrix} \begin{pmatrix} J & 1 & J_a \\ -M_J & q_1 & M_a \end{pmatrix} \times \begin{pmatrix} J_a & 1 & J_b \\ -M_a & q_2 & M_b \end{pmatrix} \begin{pmatrix} J_b & 1 & J_c \\ -M_b & q_3 & M_c \end{pmatrix} \begin{pmatrix} J_c & 1 & J \\ -M_c & q_4 & M_J \end{pmatrix}, \tag{A11}$$

$$\mathcal{C}_2 = \sum_{M_a M_c} \sum_{q_1 q_2 q_3 q_4} (-1)^{J_a-M_a+J_c-M_c} \begin{pmatrix} 1 & 1 & k_1 \\ q_1 & q_2 & 0 \end{pmatrix} \begin{pmatrix} J & 1 & J_a \\ -M_J & q_1 & M_a \end{pmatrix} \begin{pmatrix} J_a & 1 & J \\ -M_a & q_2 & M_J \end{pmatrix} \begin{pmatrix} 1 & 1 & k_2 \\ q_3 & q_4 & 0 \end{pmatrix} \times \begin{pmatrix} J & 1 & J_c \\ -M_J & q_3 & M_c \end{pmatrix} \begin{pmatrix} J_c & 1 & J \\ -M_c & q_4 & M_J \end{pmatrix}, \tag{A12}$$

where the primes over the summations in Eqs. (A9) and (A10) mean the omission of any intermediate states that are degenerate with the initial state, and the summations over intermediate states include the negative-energy states in the relativistic case. By using the graphical method of angular momentum, we can simplify $\mathcal{C}_1$ and $\mathcal{C}_2$ as

$$\mathcal{C}_1 = (-1)^{J-M_J} \begin{Bmatrix} 1 & 1 & k_1 \\ J & J_b & J_a \end{Bmatrix} \begin{Bmatrix} 1 & 1 & k_2 \\ J & J_b & J_c \end{Bmatrix} \sum_{\Lambda} (2\Lambda+1) \begin{pmatrix} J & J & \Lambda \\ -M_J & M_J & 0 \end{pmatrix} \begin{pmatrix} k_1 & k_2 & \Lambda \\ 0 & 0 & 0 \end{pmatrix} \begin{Bmatrix} k_1 & k_2 & \Lambda \\ J & J & J_b \end{Bmatrix}, \tag{A13}$$

$$\mathcal{C}_2 = \begin{pmatrix} J & J & k_1 \\ -M_J & M_J & 0 \end{pmatrix} \begin{pmatrix} J & J & k_2 \\ -M_J & M_J & 0 \end{pmatrix} \begin{Bmatrix} 1 & 1 & k_1 \\ J & J & J_a \end{Bmatrix} \begin{Bmatrix} 1 & 1 & k_2 \\ J & J & J_c \end{Bmatrix}. \tag{A14}$$

Since $\boldsymbol{\varepsilon}$ is oriented along the z axis, we can express $[\boldsymbol{\varepsilon}^{(1)} \otimes \boldsymbol{\varepsilon}^{(1)}]_0^k$ in the form

$$[\boldsymbol{\varepsilon}^{(1)} \otimes \boldsymbol{\varepsilon}^{(1)}]_0^k = \sqrt{2k+1} \begin{pmatrix} 1 & 1 & k \\ 0 & 0 & 0 \end{pmatrix} \boldsymbol{\varepsilon}^2. \tag{A15}$$

By substituting Eqs. (A13)–(A15) into Eqs. (A7) and (A8), we obtain the final expressions for $\Delta E_4^{(1)}$ and $\Delta E_4^{(2)}$:

$$\Delta E_4^{(1)} = -\varepsilon^4 \sum_{J_a J_b J_c} \mathcal{T}_1(J_a, J_b, J_c) \sum_{\lambda} (-1)^{J-M_J} \begin{pmatrix} J & J & \lambda \\ -M_J & M_J & 0 \end{pmatrix} \mathcal{G}_{\lambda}^{(1)}(J, J_a, J_b, J_c), \tag{A16}$$

$$\Delta E_4^{(2)} = \varepsilon^4 \sum_{J_a J_c} \mathcal{T}_2(J_a, J_c) \sum_{k_1 k_2} \begin{pmatrix} J & J & k_1 \\ -M_J & M_J & 0 \end{pmatrix} \begin{pmatrix} J & J & k_2 \\ -M_J & M_J & 0 \end{pmatrix} \mathcal{G}_{k_1 k_2}^{(2)}(J, J_a, J_c), \tag{A17}$$

where

$$\mathcal{G}_{\lambda}^{(1)}(J, J_a, J_b, J_c) = \sum_{k_1 k_2} (\lambda, k_1, k_2) \begin{pmatrix} 1 & 1 & k_1 \\ 0 & 0 & 0 \end{pmatrix} \begin{pmatrix} 1 & 1 & k_2 \\ 0 & 0 & 0 \end{pmatrix} \begin{pmatrix} k_1 & k_2 & \lambda \\ 0 & 0 & 0 \end{pmatrix} \begin{Bmatrix} 1 & 1 & k_1 \\ J & J_b & J_a \end{Bmatrix} \begin{Bmatrix} 1 & 1 & k_2 \\ J & J_b & J_c \end{Bmatrix} \begin{Bmatrix} k_1 & k_2 & \lambda \\ J & J & J_b \end{Bmatrix}, \tag{A18}$$

$$\mathcal{G}_{k_1 k_2}^{(2)}(J, J_a, J_c) = (k_1, k_2) \begin{pmatrix} 1 & 1 & k_1 \\ 0 & 0 & 0 \end{pmatrix} \begin{pmatrix} 1 & 1 & k_2 \\ 0 & 0 & 0 \end{pmatrix} \begin{Bmatrix} 1 & 1 & k_1 \\ J & J & J_a \end{Bmatrix} \begin{Bmatrix} 1 & 1 & k_2 \\ J & J & J_c \end{Bmatrix}, \tag{A19}$$

with the notation $(\lambda, k_1, k_2) = (2\lambda+1)(2k_1+1)(2k_2+1)$, and similarly for (k_1, k_2).

According to the properties of the $3j$ symbol, the permissible values for k_1 and k_2 in Eqs. (A18) and (A19) are 0 and 2, while the permissible values for λ are 0, 2, and 4. Also using the following formulas:

$$(-1)^{J-M_J} \begin{pmatrix} J & J & 0 \\ -M_J & M_J & 0 \end{pmatrix} = (-1)^{2J} \frac{1}{\sqrt{2J+1}}, \tag{A20}$$

$$(-1)^{J-M_J} \begin{pmatrix} J & J & 2 \\ -M_J & M_J & 0 \end{pmatrix} = (-1)^{2J} \frac{3M_J^2 - J(J+1)}{\sqrt{(2J+3)(J+1)(2J+1)J(2J-1)}}, \tag{A21}$$

$$(-1)^{J-M_J} \begin{pmatrix} J & J & 4 \\ -M_J & M_J & 0 \end{pmatrix} = (-1)^{2J} \frac{3(5M_J^2 - J^2 - 2J)(5M_J^2 + 1 - J^2) - 10M_J^2(4M_J^2 - 1)}{\sqrt{(2J+5)(J+2)(2J+3)(J+1)(2J+1)2J(2J-1)(2J-2)(2J-3)}}, \tag{A22}$$

the fourth-order energy shift ΔE_4 can finally be simplified in the form

$$\Delta E_4 = \Delta E_4^{(1)} + \Delta E_4^{(2)} = -\frac{\varepsilon^4}{24} [\gamma^{(1)} + \gamma^{(2)}], \tag{A23}$$

where

$$\gamma^{(1)} = \gamma_0^{(1)} + g_2(J, M_J)\gamma_2^{(1)} + g_4(J, M_J)\gamma_4^{(1)}, \tag{A24}$$

$$\gamma^{(2)} = \gamma_0^{(2)} + g_2(J, M_J)\gamma_2^{(2)} + g_2^2(J, M_J)\gamma_4^{(2)}. \tag{A25}$$

By denoting γ as the total hyperpolarizability, we obtain

$$\gamma = \gamma^{(1)} + \gamma^{(2)} = \gamma_0 + g_2(J, M_J)\gamma_2 + [g_4(J, M_J)\gamma_4^{(1)} + g_2^2(J, M_J)\gamma_4^{(2)}], \tag{A26}$$

where $\gamma_0 = \gamma_0^{(1)} + \gamma_0^{(2)}$, $\gamma_2 = \gamma_2^{(1)} + \gamma_2^{(2)}$, and the coefficients $g_2(J,M_J)$ and $g_4(J,M_J)$ depend also on the value of M_J:

$$g_2(J,M_J) = \begin{cases} 0, & J \le \dfrac{1}{2}, \\ \dfrac{3M_J^2 - J(J+1)}{J(2J-1)}, & \text{otherwise}, \end{cases} \tag{A27}$$

$$g_4(J,M_J) = \begin{cases} 0, & J \le \dfrac{3}{2}, \\ \dfrac{3(5M_J^2 - J^2 - 2J)(5M_J^2 + 1 - J^2) - 10M_J^2(4M_J^2 - 1)}{J(2J-1)(2J-2)(2J-3)}, & \text{otherwise}. \end{cases} \tag{A28}$$

The values of $\gamma_0^{(1)}$ and $\gamma_0^{(2)}$ correspond to the scalar components of the second hyperpolarizability, whereas $\gamma_2^{(1)}$, $\gamma_2^{(2)}$, $\gamma_4^{(1)}$, and $\gamma_4^{(2)}$ correspond to the tensor components, which have the following forms:

$$\gamma_0^{(1)} = (-1)^{2J} \frac{24}{\sqrt{2J+1}} \sum_{J_a J_b J_c} \mathcal{G}_0^{(1)}(J,J_a,J_b,J_c) \mathcal{T}_1(J_a,J_b,J_c), \tag{A29}$$

$$\gamma_2^{(1)} = (-1)^{2J} 24 \sqrt{\frac{J(2J-1)}{(2J+3)(J+1)(2J+1)}} \sum_{J_a J_b J_c} \mathcal{G}_2^{(1)}(J,J_a,J_b,J_c) \mathcal{T}_1(J_a,J_b,J_c), \tag{A30}$$

$$\gamma_4^{(1)} = (-1)^{2J} 24 \sqrt{\frac{J(2J-1)(J-1)(2J-3)}{(2J+5)(J+2)(2J+3)(J+1)(2J+1)}} \sum_{J_a J_b J_c} \mathcal{G}_4^{(1)}(J,J_a,J_b,J_c) \mathcal{T}_1(J_a,J_b,J_c), \tag{A31}$$

$$\gamma_0^{(2)} = -\frac{24}{2J+1} \sum_{J_a J_c} \mathcal{G}_{00}^{(2)}(J,J_a,J_c) \mathcal{T}_2(J_a,J_c), \tag{A32}$$

$$\gamma_2^{(2)} = -\frac{24}{2J+1} \sqrt{\frac{J(2J-1)}{(2J+3)(J+1)}} \sum_{J_a J_c} [\mathcal{G}_{02}^{(2)}(J,J_a,J_c) + \mathcal{G}_{20}^{(2)}(J,J_a,J_c)] \mathcal{T}_2(J_a,J_c), \tag{A33}$$

$$\gamma_4^{(2)} = -\frac{24J(2J-1)}{(2J+3)(2J+1)(J+1)} \sum_{J_a J_c} \mathcal{G}_{22}^{(2)}(J,J_a,J_c) \mathcal{T}_2(J_a,J_c). \tag{A34}$$

In the nonrelativistic case, we only need to substitute the total angular quantum number J with the orbital angular quantum number L, and replace the magnetic quantum number M_J with M_L.

Appendix B: Convergence test for excited states of the H atom

Table B1. Convergence of the nonrelativistic pure state hyperpolarizabilities γ_0, γ_2, and $\gamma_4^{(2)}$ for the 2p state of the H atom, in atomic units.

N	$10^{-6}\gamma_0$	$10^{-6}\gamma_2$	$10^{-4}\gamma_4^{(2)}$
100	8.130 559 999 999 999 42	−2.769 471 999 999 997 9	−3.423 999 999 999 996 7
150	8.130 559 999 999 999 996 5	−2.769 471 999 999 999 987	−3.423 999 999 999 999 981
200	8.130 559 999 999 999 999 899	−2.769 471 999 999 999 999 64	−3.423 999 999 999 999 999 47
250	8.130 559 999 999 999 999 993 5	−2.769 471 999 999 999 999 977	−3.423 999 999 999 999 999 966
300	8.130 559 999 999 999 999 999 30	−2.769 471 999 999 999 999 997 5	−3.423 999 999 999 999 999 996 4
350	8.130 559 999 999 999 999 999 89	−2.769 471 999 999 999 999 999 62	−3.423 999 999 999 999 999 999 45
400	8.130 559 999 999 999 999 999 98	−2.769 471 999 999 999 999 999 93	−3.423 999 999 999 999 999 999 89
Extrap.	8.130 560	−2.769 472	−3.424 0

Table B2. Convergence of the nonrelativistic pure state hyperpolarizabilities γ_0, γ_2, $\gamma_4^{(1)}$, and $\gamma_4^{(2)}$ for the 3d state of the H atom, in atomic units.

N	$10^{-9}\gamma_0$	$10^{-9}\gamma_2$	$10^{-7}\gamma_4^{(1)}$	$10^{-7}\gamma_4^{(2)}$
100	1.913 524 179 299 999 1	−1.027 110 959 357 141 8	2.939 248 330 714 278	−6.944 162 399 999 999 0
150	1.913 524 179 299 999 995	−1.027 110 959 357 142 851	2.939 248 330 714 285 67	−6.944 162 399 999 999 994
200	1.913 524 179 299 999 999 85	−1.027 110 959 357 142 857 0	2.939 248 330 714 285 713	−6.944 162 399 999 999 999 85
250	1.913 524 179 299 999 999 991	−1.027 110 959 357 142 857 13	2.939 248 330 714 285 714 20	−6.944 162 399 999 999 999 990
300	1.913 524 179 299 999 999 999 0	−1.027 110 959 357 142 857 141 6	2.939 248 330 714 285 714 277	−6.944 162 399 999 999 999 999 0
350	1.913 524 179 299 999 999 999 85	−1.027 110 959 357 142 857 142 7	2.939 248 330 714 285 714 284	−6.944 162 399 999 999 999 999 85
400	1.913 524 179 299 999 999 999 97	−1.027 110 959 357 142 857 142 8	2.939 248 330 714 285 714 285	−6.944 162 399 999 999 999 999 97
Extrap	1.913 524 179 3	−1.027 110 959 357 142 857 142 8	2.939 248 330 714 285 714 286	−6.944 162 4

Table B3. Convergence of the relativistic pure state hyperpolarizabilities γ_0, γ_2, and $\gamma_4^{(2)}$ for the $2p_{1/2}$ and $2p_{3/2}$ states of the H atom, in atomic units.

N	$2p_{1/2}$	$2p_{3/2}$		
	$10^{-6}\gamma_0$	$10^{-6}\gamma_0$	$10^{-6}\gamma_2$	$10^{-4}\gamma_4^{(2)}$
100	8.129 480 180 856	8.130 501 053 31	−2.769 565 818 758	−3.424 116 618 84
200	8.129 480 180 847 221	8.130 501 053 270 538 9	−2.769 565 818 725 861	−3.424 116 618 636 726 0
300	8.129 480 180 847 218 663	8.130 501 053 270 535 691	−2.769 565 818 725 858 675	−3.424 116 618 636 721 347
400	8.129 480 180 847 218 657 977	8.130 501 053 270 535 680 91	−2.769 565 818 725 858 667 51	−3.424 116 618 636 721 334 86
500	8.129 480 180 847 218 657 893	8.130 501 053 270 535 680 760	−2.769 565 818 725 858 667 395	−3.424 116 618 636 721 334 673
600	8.129 480 180 847 218 657 892	8.130 501 053 270 535 680 756	−2.769 565 818 725 858 667 393	−3.424 116 618 636 721 334 669
Extrap.	8.129 480 180 847 218 657 892	8.130 501 053 270 535 680 756	−2.769 565 818 725 858 667 393	−3.424 116 618 636 721 334 669

Table B4. Convergence of the relativistic hyperpolarizabilities pure state γ_0, γ_2, and $\gamma_4^{(2)}$ for the $3d_{3/2}$ state of the H atom, in atomic units.

N	$10^{-9}\gamma_0$	$10^{-8}\gamma_2$	$10^{-7}\gamma_4^{(2)}$
100	1.913 481 814 79	−7.189 813 884	−3.402 556 954 7
200	1.913 481 814 288 678	−7.189 813 879 847 98	−3.402 556 953 695 364
300	1.913 481 814 288 667 955	−7.189 813 879 847 891 83	−3.402 556 953 695 351 874
400	1.913 481 814 288 667 929 1	−7.189 813 879 847 891 586 0	−3.402 556 953 695 351 845 92
500	1.913 481 814 288 667 928 69	−7.189 813 879 847 891 582 22	−3.402 556 953 695 351 845 49
600	1.913 481 814 288 667 928 68	−7.189 813 879 847 891 582 07	−3.402 556 953 695 351 845 47
Extrap.	1.913 481 814 288 667 928 67	−7.189 813 879 847 891 582 06	−3.402 556 953 695 351 845 47

Table B5. Convergence of the relativistic pure state hyperpolarizabilities γ_0, γ_2, $\gamma_4^{(1)}$, and $\gamma_4^{(2)}$ for the $3d_{5/2}$ state of the H atom, in atomic units.

N	$10^{-9}\gamma_0$	$10^{-9}\gamma_2$	$10^{-7}\gamma_4^{(1)}$	$10^{-7}\gamma_4^{(2)}$
100	1.913 513 569 27	−1.027 113 325 40	2.939 326 813 538	−6.944 098 826 2
200	1.913 513 569 010 927 2	−1.027 113 325 161 428 2	2.939 326 812 562 20	−6.944 098 825 526 127
300	1.913 513 569 010 920 534	−1.027 113 325 161 421 963	2.939 326 812 562 169 80	−6.944 098 825 526 114 456
400	1.913 513 569 010 920 516 1	−1.027 113 325 161 421 946 33	2.939 326 812 562 169 713 4	−6.944 098 825 526 114 424 88
500	1.913 513 569 010 920 515 82	−1.027 113 325 161 421 946 06	2.939 326 812 562 169 711 98	−6.944 098 825 526 114 424 39
600	1.913 513 569 010 920 515 81	−1.027 113 325 161 421 946 05	2.939 326 812 562 169 711 92	−6.944 098 825 526 114 424 37
Extrap.	1.913 513 569 010 920 515 81	−1.027 113 325 161 421 946 05	2.939 326 812 562 169 711 92	−6.944 098 825 526 114 424 37

Acknowledgements

This work was supported by the National Natural Science Foundation of China (Grant Nos. 12174402 and 12393821), the Strategic Priority Research Program of the Chinese Academy of Sciences (Grant Nos. XDB0920100 and XDB0920101), and the Nature Science Foundation of Hubei Province (Grant Nos. 2019CFA058 and 2022CFA013). ZCY was supported by the Natural Sciences and Engineering Research Council of Canada (NSERC). JFB was supported in part by NSF grant PHY-2116679. All the calculations are finished on the APM-Theoretical Computing Cluster (APM-TCC).

References

[1] Mitroy J, Safronova M S and Clark Charles W 2010 *J. Phys. B: At. Mol. Opt. Phys.* **43** 202001
[2] Tang L Y, Zhang Y H, Zhang X Z, Jiang J and Mitroy J 2012 *Phys. Rev. A* **86** 012505
[3] Zhang Y H, Tang L Y, Zhang X Z and Shi T Y 2015 *Phys. Rev. A* **92** 012515
[4] Zhang Y H, Tang L Y, Zhang X Z and Shi T Y 2016 *Chin. Phys. B* **25** 103101
[5] Tang L Y, Yan Z C, Shi T Y and Mitroy J 2010 *Phys. Rev. A* **81** 042521
[6] Bishop D M and Pipin J 1995 *Chem. Phys. Lett.* **236** 15
[7] Thakkar A J and Lupinetti C 2006 *Atomic, Molecules and Clusters in Electric Field: Theoretical Approaches to the Calculation of Electric Polarizability*, edited by G. Maroulis (London: Imperial College)
[8] Shelton D P and Rice J E 1994 *Chem. Rev.* **94** 3
[9] Manakov N L, Marmo S I and Fainshtein A G 1986 *Zh. Eksp. Teor. Fiz.* **91** 51
[10] Manakov N L, Ovsiannikov V D and Rapoport L P 1986 *Phys. Rep.* **141** 320
[11] Henson B M, Ross J A, Thomas K F, Kuhn C N, Shin D K, Hodgman S S, Zhang Y H, Tang L Y, Drake G W F, Bondy A T, Truscott A G and Baldwin K G H 2022 *Science* **376** 199
[12] Yang J, He X, Guo R, Xu P, Wang K, Sheng C, Liu M, Wang J, Derevianko A and Zhan M 2016 *Phys. Rev. Lett.* **117** 123201
[13] Sheng C, He X, Xu P, Guo R, Wang K, Xiong Z, Liu M, Wang J and Zhan M 2018 *Phys. Rev. Lett.* **121** 240501
[14] Guo R, He X, Sheng C, Yang J, Xu P, Wang K, Zhong J, Liu M, Wang J and Zhan M 2020 *Phys. Rev. Lett.* **124** 153201
[15] Nicholson T L, Campbell S L, Hutson R B, Marti G E, Bloom B J, McNally R L, Zhang W, Barrett M D, Safronova M S, Strouse G F, Tew W L and Ye J 2015 *Nat. Commun.* **6** 6896
[16] Brown R C, Phillips N B, Beloy K, McGrew W F, Schioppo M, Fasano R J, Milani G, Zhang X, Hinkley N, Leopardi H, Yoon T H, Nicolodi D, Fortier T M and Ludlow A D 2017 *Phys. Rev. Lett.* **119** 253001
[17] Ushijima I, Takamoto M and Katori H 2018 *Phys. Rev. Lett.* **121** 263202
[18] Kim K, Aeppli A, Bothwell T and Ye J 2023 *Phys. Rev. Lett.* **130** 113203
[19] Bohorquez J C, Chinnarasu R, Isaacs J, Booth D, Beck M, McDermott R and Saffman M 2023 *Phys. Rev. A* **108** 022805
[20] Tang L Y, Yan Z C, Shi T Y and Babb James F 2009 *Phys. Rev. A* **79** 062712
[21] Jhanwar B L and Meath W J 1980 *Mol. Phys.* **40** 713
[22] Tang L Y, Zhang J Y, Yan Z C, Shi T Y, Babb James F and Mitroy J 2009 *Phys. Rev. A* **80** 042511
[23] Tiesinga E, Mohr P J, Newell D B and Taylor B N 2021 *Rev. Mod. Phys.* **93** 025010

[24] S. Kaneko 1977 *J. Phys. B: Atom. Mol. Phys.* **10** 3347
[25] Johnson W R, Blundell S A and Sapirstein J 1988 *Phys. Rev. A* **37** 307
[26] Fischer C F and Parpia F A 1993 *Phys. Lett. A* **179** 198
[27] Bachau H, Cormier E, Decleva P, Hansen J E and Martín F 2001 *Rep. Prog. Phys.* **64** 1815
[28] Chodos A, Jaffe R L, Johnson K, Thorn C B and Weisskopf V F 1974 *Phys. Rev. D* **9** 3471
[29] Bethe H A and Salpeter E E 1977 *Quantum Mechanics of One- and Two-Electron Atoms* (New York: Plenum)
[30] Tang Y B, Qiao H X, Shi T Y and Mitroy J 2013 *Phys. Rev. A* **87** 042517
[31] Jiang J, Mitroy J, Cheng Y and Bromley Michael W J 2016 *Phys. Rev. A* **94** 062514
[32] Wu F F, Tang Y B, Shi T Y and Tang L Y 2019 *Phys. Rev. A* **100** 042514
[33] Johnson W R, Kolb D and Huang K N 1983 *At. Data Nucl. Data Tables* **28** 333
[34] Bishop D M and Pipin J 1992 *J. Chem. Phys.* **97** 3375
[35] Cohen S and Themelis S I 2006 *J. Chem. Phys.* **124** 134106
[36] Kramida A, Ralchenko Yu, Reader J and NIST ASD Team 2023 *NIST Atomic Spectra Database* (version 5.11) https://physics.nist.gov/asd
[37] Barakhshan P, Marrs A, Bhosale A, Arora B, Eigenmann R and Safronova M S 2022 *Portal for High-Precision Atomic Data and Computation* (version 2.0) https://www.udel.edu/atom
[38] Safronova U I and Safronova M S 2013 *Phys. Rev. A* **87** 032502
[39] Kolb D, Johnson W R and Shorer P 1982 *Phys. Rev. A* **26** 19
[40] Singh S, Kaur M, Arora B and Sahoo B K 2018 *Phys. Rev. A* **98** 013406